DOI: 10.61782/fa.2023.0831

forum acusticum 2023

SHAPE OPTIMIZATION OF RECTANGULAR ACOUSTIC BLACK HOLES WITH INSERTION OF POROUS MATERIALS

Aneta Furmanová[1], **Viktor Hruška**[1*], **Milan Červenka**[1], **Jean-Philippe Groby**[2], **Michal Bednařík**[1]

[1] Czech Technical University in Prague, Faculty of Electrical Engineering, Technická 2, 166 27, Prague 6, Czech Republic

[2] Laboratoire d'Acoustique de l'Université du Mans (LAUM), UMR 6613, Institut d'Acoustique - Graduate School (IA-GS), CNRS, Le Mans Université, France

ABSTRACT

The goal of this research is to enhance sound absorption in rectangular acoustic black holes (ABHs), also known as metamaterial graded absorbers, by optimizing their design using evolutionary algorithms, specifically the covariance matrix adaptation evolution strategies (CMA-ES). The designs must have good practical feasibility for 3D printing. A model based on the Riccati equation is employed to optimize the reflection coefficient of the rectangular ABH. The shape of the ABH profile is controlled by a high-order Bézier curve, providing greater flexibility than simpler profiles such as polynomials. Additionally, the study explores the use of porous material and the optimization of its macroscopic geometry. Results demonstrate that the use of ABHs can significantly improve sound absorption in a frequency range below the Biot frequency of the porous material.

Keywords: *acoustic black hole, porous materials, evolution strategy optimization*

1. INTRODUCTION

In 2002, Mironov and Pisylakov [1] published a concept of sound attenuating device for acoustic waves in air based on the gradual reduction of the sound speed for which the term acoustic black hole (ABH) was adopted (see e.g., [2] for a recent review). The most typical realization consists of a waveguide termination into which a series of thin obstacles (either rectangular plates or axis-symmetric rings) is embedded, thus forming a locally reacting effective impedance wall (see Fig. 1). Nomenclature analogy with astrophysics is based on an asymptotic application of the original theory, in which the impinging wave could not reach the end of the structure in finite time and as a consequence there would be no reflection.

However, this model behavior is based on assumptions that cannot be fulfilled in the real world, which is nowadays well documented experimentally [1, 3–6]. In practice, slowing down the wave results in increasing of the acoustic energy density, which in turn increases the effect of otherwise weak dissipation mechanisms, such as thermoviscous losses at the walls within the ABH slits (see e.g., [2, 7, 8]).

It follows that the key issue in describing the quasi-plane wave propagation within the ABH is the right model of energy dissipation. While Mironov and Pislyakov [1] initially added only a small imaginary part to the sound speed to account for losses, this approach was found to be limited in its ability to capture the underlying physics [7]. Beside that, there were more effective solutions, such as an equivalent metafluid by Guasch et al. [9] or a framework inspired by porous materials by Umnova et al. [10].

An additional dissipation mechanism is often necessary to achieve broadband absorption. For this purpose micro-perforated plates covering the slits [11], melamine foam [8], sponges [3], or combination of porous material with metamaterial matching [12] were employed. In

*Corresponding author: viktor.hruska@fel.cvut.cz.

this text, we consider the optimization of the ABH geometry along with the appropriate use of porous material. The material is described as an effective fluid with the Johnson-Champoux-Allard-Lafarge (JCAL) model ([13] and see e.g., [14] for state of the art summary).

Our approach based on the solution of the Riccati equation is sufficiently variable and transparent to allow for a more general parameterization of the profile function using Bézier curves. In the following we only consider geometries that can be easily 3D printed with the current state of available resources (i.e. we purposely do not account for the possibility of further 3D printing evolution).

The paper is organized as follows. First, the outline of the theory and governing equations are given in Section 2, along with the proposed optimization procedure. Next, in Section 3, the results of optimization are presented. Possible occurence of another related phenomena is discussed in Section 4 and finally some conclusions are drawn in Section 5.

2. THEORY

In this section, we describe the parametrization of the ABH geometry and the equation of Riccati type governing the wave propagation within the structure. Finally, an outline of the optimization algorithm is given.

We consider rectangular ABH of the height $2A$ and length L. Hence, the cross-section of the device is $2A \times B$, where we suppose $B \leq 2A$. It follows that the cut-on frequency of the waveguide is $f_{\text{cut}} = c_0/(4A)$. Heights of the ribs are given by function $\ell(x) = A - a(x)$, where $a(x)$ is the profile function. The spatial period W is the sum of slit width and the rib width. The width of slits is described as $w = \xi W$, where $\xi \in (0, 1)$ is the rib-width to slit ratio; and the rib-width as $(1 - \xi)W$. For the illustration of the considered ABH, see Fig. 1.

2.1 Riccati equation

The original theory [1] is based on the generalized Webster equation for acoustic pressure. It is well-established that a whole class of such wave equations with spatial inhomogeneity can be transformed into the Riccati equation for reflection coefficient R (see e.g. [10, 15]). This approach is employed below. In order to use the quasi-plane-wave approximation, the frequency of a harmonic propagating wave should be lower than f_{cut}. For the rectangular ABH the Riccati equation takes the form:

$$\begin{aligned}\frac{\mathrm{d}R}{\mathrm{d}x} = &\left(-\frac{1}{2a}\frac{\mathrm{d}a}{\mathrm{d}x} - \frac{\rho_0 c_0 Y_w}{2a} + F_{\nu,1}(\omega, x)\right) R^2 \\ &- \left(\mathrm{j}2k_0 + \frac{\rho_0 c_0 Y_w}{a} + F_{\nu,2}(\omega, x)\right) R \\ &+ \left(\frac{1}{2a}\frac{\mathrm{d}a}{\mathrm{d}x} - \frac{\rho_0 c_0 Y_w}{2a} + F_{\nu,1}(\omega, x)\right) ,\end{aligned} \tag{1}$$

where $a = a(x)$, ρ_0, $\omega = 2\pi f$, c_0, $k_0 = \omega/c_0$, $F_{\nu,1,2}$, $\mathrm{j} = \sqrt{-1}$, are the profile function, fluid ambient density, angular frequency, adiabatic sound speed, wavenumber, functions governing the thermoviscous losses in the bulk of the ABH, and the imaginary unit, respectively. The varying wall admittance $Y_w = Y_w(x, \omega)$ is given by

$$Y_w(x, \omega) = \frac{\mathrm{j}\xi}{\rho_{\text{eff}} c_{\text{eff}}} \tan\left(\frac{\omega}{c_{\text{eff}}}\ell\right) , \tag{2}$$

where effective sound speed $c_{\text{eff}} = c_{\text{eff}}(\omega, w)$ and effective unperturbed material density $\rho_{\text{eff}} = \rho_{\text{eff}}(\omega, w)$ in the slits are given by Stinson's model [16] for air-filled slits, or by Johnson-Champoux-Allard-Lafarge (JCAL) Model [17] for slits filled with porous material.

It is worth noting that for given material parameters the coefficients of Eq. (1) actually vary only with the profile function $a(x)$ and frequency.

2.2 Optimization

2.2.1 *Object of optimization and cost function*

In this work, we do not focus on optimizing the parameters of porous materials, but on using the ABH geometry to maximize the effect of the porous material. Therefore, we have chosen one of the preferred uses of porous materials as a benchmark. Namely, the waveguide termination in length of a quarter-wavelength resonance at the Biot frequency [18]

$$f_{\text{Biot}} = \frac{\sigma\phi}{2\pi\rho_0\alpha_\infty} , \tag{3}$$

where σ, ϕ, ρ_0, α_∞ are the flow resistivity, porosity, density of the saturating fluid and tortuosity, respectively [18]. We are mainly interested in a frequency region below the Biot frequency of the porous material, i.e., we would like to outperform the porous material in its viscous regime. Hence, the cost function is proposed as maximization of

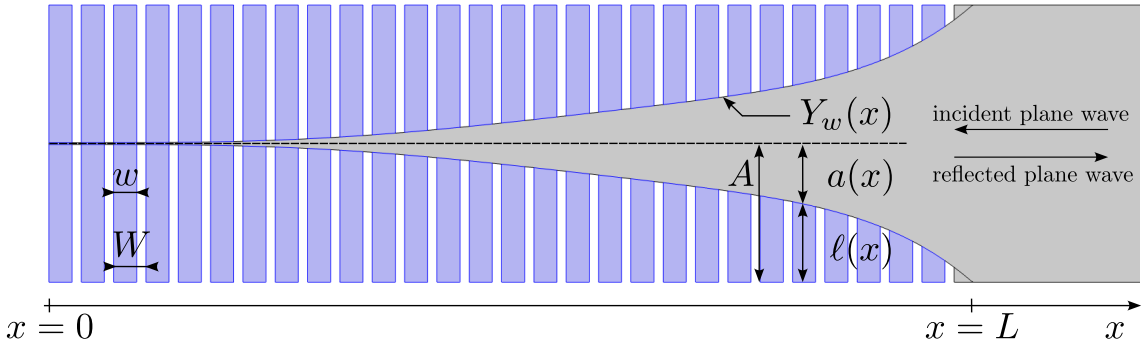

Figure 1. Profile diagram of the considered rectangular ABH terminated by a perfectly rigid wall (porous material marked in blue). The depicted geometry corresponds to the optimal solution from Sec. 3.1.

the surface area under the absorption coefficient spectra α of the particular offspring:

$$\frac{1}{f_{\text{Biot}}} \int_0^{f_{\text{Biot}}} \alpha(f) \mathrm{d}f \ , \tag{4}$$

where the absorption coefficient $\alpha(f)$ is calculated as $\alpha(f) = 1 - R^2(f)$.

2.2.2 *Geometry and algorithm*

The reflection coefficient spectrum $R(x = L, \omega)$ is influenced by many parameters. Since the ABH is usually a termination of a more complex device, due to practical feasibility and in order to fit in geometry requirements, we consider the height $2A$, length L, width of slit w and spatial period of ribs W as given.

Our subject of the optimization is the profile function $a(x)$, which should be a continuous, smooth, slowly varying curve. For such type of curves, a Bézier curve parametrisation is widely used. Because the Bézier curve domain is $[0, 1]$, it is needed to adopt a profile function normalization by the ABH length L, so the length of ABH becomes 1 and the half-height is A/L, see Fig. 2.

The Bézier curve of n-th order is defined for a set of $n + 1$ control points $\mathbf{P}_0$, $\mathbf{P}_1$, $\mathbf{P}_2$, ..., $\mathbf{P}_n$. Two restrictions are introduced for clarity and simplicity. Firstly, let the points $\mathbf{P}_i = (x_i, y_i)$ be equidistantly distributed along the x-axis and only the y-coordinate be variable. Furthermore, let the endpoint $\mathbf{P}_n$ be fixed as $\mathbf{P}_n = (1, 0)$, because otherwise, it may cause unwanted impedance mismatch at the entry of ABH. Therefore, the parameters to be optimized, are the control points $\mathbf{P}_0, \mathbf{P}_1, \mathbf{P}_2, ..., \mathbf{P}_{n-1}$. The exact number of necessary control points is a priori unknown. In practice, we start with lower amount and restart the optimization with increasing number of control points until convergence (where the outcome of the previous optimization step serves as the initial guess for the subsequent one).

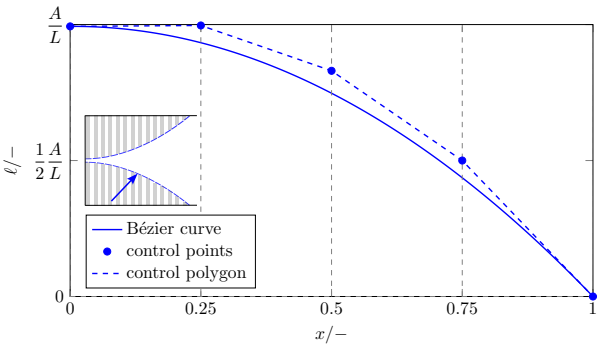

Figure 2. A Bézier curve adapted to the geometry of ABH

Since the relationship between the profile function a and the reflection coefficient spectra is complicated, we use a derivative-free optimization. The Covariance Matrix Adaptation Evolution Strategy (CMA-ES) was chosen as a suitable method for optimizing a nonlinear function with unknown search space. The optimization algorithm was implemented using the open-source Python library for CMA Evolution Strategy [19], together with libraries NumPy [20] and SciPy [21].

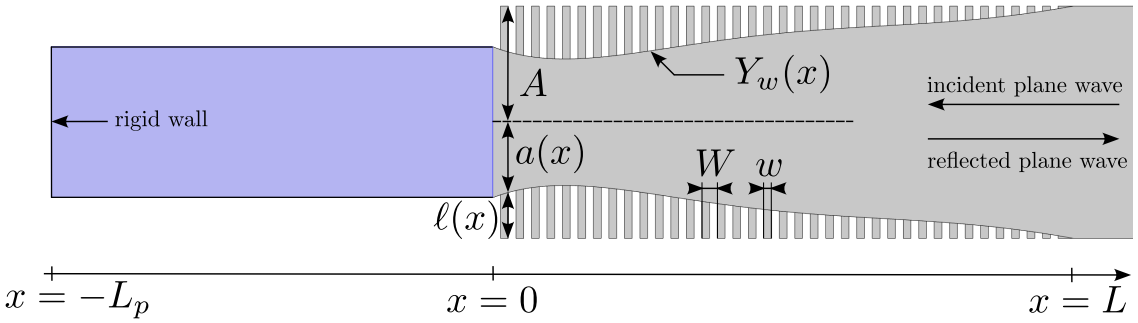

Figure 3. Profile diagram of the considered rectangular ABH terminated by a porous material (marked in blue). The depicted geometry corresponds to the optimal solution from Sec. 3.2.

3. RESULTS

Throughout this text, we consider the following values of material quantities (air in our case): adiabatic sound speed $c_0 = 343\ \mathrm{m\,s^{-1}}$, air density $\rho_0 = 1.2\ \mathrm{kg\,m^{-3}}$, dynamic viscosity $\mu = 1.83 \times 10^{-5}\ \mathrm{Pa\,s}$, adiabatic exponent $\gamma = 1.4$, specific heat capacity at constant pressure $c_p = 1004\ \mathrm{J\,kg^{-1}\,K^{-1}}$, thermal conductivity $\varkappa = 2.59\ \mathrm{W\,m^{-1}\,K^{-1}}$ and the Prandtl number $\mathrm{Pr} = 0.71$. The adiabatic bulk modulus is given as $K_0 = \gamma P_0$, where $P_0 = \rho_0 c_0^2/\gamma$ is the static pressure.

The parameters of chosen porous material are following: flow resistivity $\sigma = 5678\ \mathrm{Pa\,s\,m^{-2}}$, porosity $\phi = 0.99$, tortuosity $\alpha_\infty = 1$, static viscous permeability $\kappa_0 = 3.1877 \times 10^{-9}\ \mathrm{m^2}$, static thermal permeability $\kappa_0' = 4.5866 \times 10^{-9}\ \mathrm{m^2}$, thermal and viscous characteristic lengths $\Lambda' = 244\ \mu\mathrm{m}$ and $\Lambda = 147\ \mu\mathrm{m}$, respectively.

The Biot frequency for this porous material is $f_{\mathrm{Biot}} = 752$ Hz, therefore the length of the quarter-wavelength resonator is $L_p = 11.4$ cm. For the optimization, a ABH with height $2A = 6$ cm was considered, thus the cut-on frequency for this given case is $f_{\mathrm{cut}} = 2858$ Hz. Note, that in our case, the Biot frequency is significantly lower than the cut-on frequency, $f_{\mathrm{Biot}} < f_{\mathrm{cut}}$, and therefore, the condition for plane-wave approximation is fulfilled.

For validation, we simulated the optimized results using the finite element method (FEM). Specifically, our simulations were done in Comsol Multiphysics 5.5 (Pressure Acoustics, Frequency domain study with JCAL model for porous material parts).

3.1 ABH terminated by a porous material

We first studied a configuration in which the rigid termination was replaced by porous material. Our strategy was to use a porous termination at the length corresponding to the quarter-wavelength resonance at the Biot frequency and try to improve the absorption by using ABH (making use of energy density concentration and impedance matching).

In this case, ABH of length $L = 15$ cm terminated by porous material of length $L_p = 11.4$ cm was considered, with width of the slits $w = 2$ mm and the same width of ribs.

The optimal shape for this task is depicted in Fig. 3. Clearly, it is advantageous to leave the ABH profile at $x = 0$ wide open, exposing the wave to large area of porous material with rather moderate concentration due to the ABH shape. The absorption coefficient is depicted in Fig. 4. Employing this optimal design it is possible to reach $\alpha > 0.9$ about 100 Hz before the benchmark case.

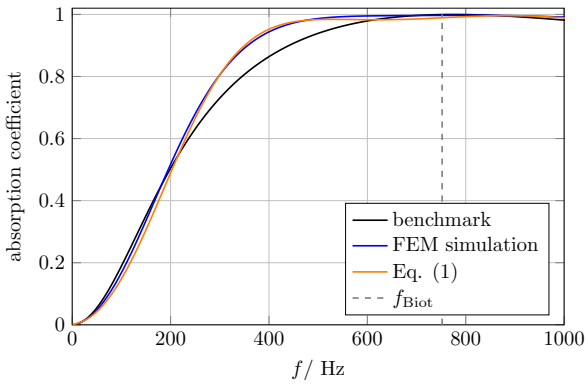

Figure 4. Absorption coefficient for the ABH terminated by a porous material (see Fig. 3).

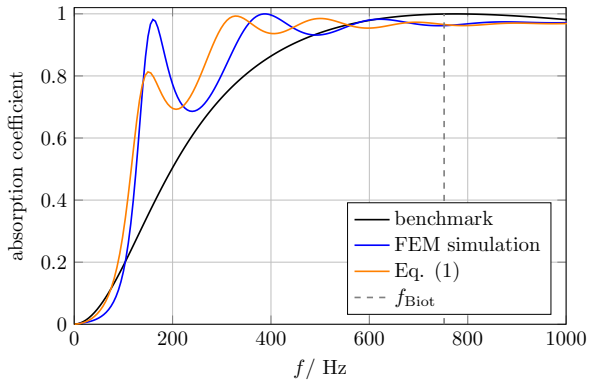

Figure 5. Absorption coefficient for the ABH employing slits filled with porous material (see Fig. 1).

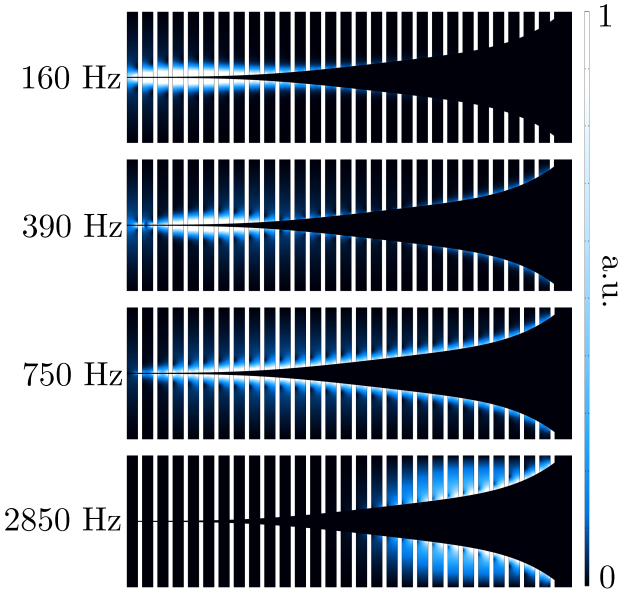

Figure 6. Estimation of power losses in slits filled with porous material at different frequencies. The depicted quantity is $-2|\boldsymbol{i}|\mathrm{Im}(k)$, where $|\boldsymbol{i}|$ and k denote magnitude of the acoustic intensity vector and the complex wavenumber, respectively.

3.2 ABH employing slits filled with porous material

The second possibility studied here is the filling of slits with porous material. To do this, the geometry had to be changed. Specifically, it is necessary to make the slits wider because of the typical pore size. Thus, in this optimization we have the total length $L = 20$ cm and the width of the slits $w = 5$ mm and the width of ribs 2 mm.

The optimal shape for this configuration is depicted in Fig. 1 and the corresponding absorption coefficient α in Fig. 5. In this case, the qualitative behavior is more complicated than in the previous one. The absorption peaks are presumably on the frequencies for which the conditions for critical coupling are met (see e.g., [22–24]). In overall, we achieve $\alpha > 0.7$ already for a frequency corresponding to $\approx f_{\text{Biot}}/5$.

To shed more light on functioning in this case, the estimation of losses in different parts of ABH and for different frequencies is depicted in Fig. 6. It is evident that for lower frequencies the majority of sound energy dissipation takes place at the closed end of the ABH and with increasing frequency this location moves toward the ABH's open end. In higher frequency range, the wave energy does not even reach the closed end as already noted in [7] in a similar case.

4. DISCUSSION

We have focused on absorption below the Biot frequency of the porous material, i.e. in its viscous regime. This is based on the assumption that porous materials above this threshold generally perform well. However, especially for the ABH terminated with porous material, we have seen some instances where this might not be the case. For reasons of scope, we do not discuss this issue here. However, we have been able to suppress it by changes in the cost function (e.g., by extending its frequency range with appropriate weights).

In fact, for the optimization in Section 3.2 we used a more general wall function Y_w allowing only partial filling of the slit with porous material. However, none of the optimal solutions used this option and Eq. (1) suffices, so we omitted the more complex formula for brevity.

Differences between the FEM simulation and the results of Eq. (1) are likely to be due to absence of specific phenomena in the quasi-onedimensional approach, such as evanescent coupling, length corrections for the radiation from slits into the main waveguide etc. However, it follows from Figs. 4, 5 that the computationally cheap 1D model performs good in comparison with FEM simulation even when the number of slits per ABH length is relatively low.

5. CONCLUSIONS

In this work, we have studied two possible ways to employ porous material within the ABH for sound waves in air. The goal was to outperform the chosen benchmark: the waveguide termination by the porous material whose thickness corresponds to a quarter wavelength resonator at the Biot frequency.

In the first configuration, the porous material replaced the rigid end of the ABH structure (see Fig. 3). In this configuration, it manages to outperform the benchmark, but the overall benefit is questionable: the advantages of energy concentration and some impedance matching probably do not outweigh the increase in overall length, nor are there significant savings in porous material consumption.

The second possible configuration consisted of partial or complete filling of the ABH slits with porous material (see Fig. 1). Here we have succeeded in extending the frequency range of efficient absorption ($\alpha > 0.7$ from 140 Hz, which corresponds to $\approx f_{\text{Biot}}/5$). Moreover, there are two peaks corresponding to almost perfect absorption in the frequency range below f_{Biot}.

The results of this work provide a solid basis for future experimental validation, as well as for the use of other types of porous materials (e.g. felts to name one).

6. ACKNOWLEDGMENTS

This work was supported by the Grant Agency of the Czech Republic (GACR) grant No. 22-33896S. Viktor Hruška and Jean-Philippe Groby would like to thank the support of the Agence Nationale de la Recherche via the grant ANR 17-EURE-0014.

7. REFERENCES

[1] M. A. Mironov and V. V. Pislyakov, "One-dimensional acoustic waves in retarding structures with propagation velocity tending to zero," *Acoustical Physics*, vol. 48, pp. 347–352, May 2002.

[2] A. Pelat, F. Gautier, S. C. Conlon, and F. Semperlotti, "The acoustic black hole: A review of theory and applications," *Journal of Sound and Vibration*, vol. 476, p. 115316, June 2020.

[3] A. Azbaid El Ouahabi, V. Krylov, and D. O'Boy, "Experimental investigation of the acoustic black hole for sound absorption in air," in *22nd International Congress on Sound and Vibration, Florence, Italy*, 07 2015.

[4] A. Azbaid El Ouahabi, V. Krylov, and D. O'Boy, "Investigation of the acoustic black hole termination for sound waves propagating in cylindrical waveguides," in *International Conference 'InterNoise 2015', San Francisco, USA*, 08 2015.

[5] M. Mironov and V. Pislyakov, "One-dimensional sonic black holes: Exact analytical solution and experiments," *Journal of Sound and Vibration*, vol. 473, p. 115223, May 2020.

[6] Y. Mi, W. Zhai, L. Cheng, C. Xi, and X. Yu, "Wave trapping by acoustic black hole: Simultaneous reduction of sound reflection and transmission," *Applied Physics Letters*, vol. 118, p. 114101, Mar. 2021.

[7] M. Červenka and M. Bednařík, "On the role of resonance and thermoviscous losses in an implementation of "acoustic black hole" for sound absorption in air," *Wave Motion*, vol. 114, p. 103039, Sept. 2022.

[8] A. Mousavi, M. Berggren, and E. Wadbro, "How the waveguide acoustic black hole works: A study of possible damping mechanisms," *The Journal of the Acoustical Society of America*, vol. 151, pp. 4279–4290, June 2022.

[9] O. Guasch, P. Sánchez-Martín, and D. Ghilardi, "Application of the transfer matrix approximation for wave propagation in a metafluid representing an acoustic black hole duct termination," *Applied Mathematical Modelling*, vol. 77, pp. 1881–1893, Jan. 2020.

[10] O. Umnova, D. Brooke, P. Leclaire, and T. Dupont, "Multiple resonances in lossy acoustic black holes - theory and experiment," *Journal of Sound and Vibration*, vol. 543, p. 117377, Jan. 2023.

[11] X. Zhang and L. Cheng, "Broadband and low frequency sound absorption by sonic black holes with micro-perforated boundaries," *Journal of Sound and Vibration*, vol. 512, p. 116401, Nov. 2021.

[12] A. S. Elliott, R. Venegas, J. P. Groby, and O. Umnova, "Omnidirectional acoustic absorber with a porous core and a metamaterial matching layer," *Journal of Applied Physics*, vol. 115, p. 204902, May 2014.

[13] D. Lafarge, P. Lemarinier, J. F. Allard, and V. Tarnow, "Dynamic compressibility of air in porous structures at audible frequencies," *The Journal of the Acoustical Society of America*, vol. 102, pp. 1995–2006, Oct. 1997.

[14] N. Jimenez, O. Umnova, and J.-P. Groby, eds., *Acoustic waves in periodic structures, metamaterials, and porous media*. Topics in applied physics, Cham, Switzerland: Springer Nature, 1 ed., Nov. 2021.

[15] L. D. Ryck, W. Lauriks, P. Leclaire, J. P. Groby, A. Wirgin, and C. Depollier, "Reconstruction of material properties profiles in one-dimensional macroscopically inhomogeneous rigid frame porous media in the frequency domain," *The Journal of the Acoustical Society of America*, vol. 124, pp. 1591–1606, Sept. 2008.

[16] M. R. Stinson, "The propagation of plane sound waves in narrow and wide circular tubes, and generalization to uniform tubes of arbitrary cross-sectional shape," *J. Acoust. Soc. Am.*, vol. 89, pp. 550–558, 1991.

[17] N. Jiménez, J.-P. Groby, and V. Romero-García, *The Transfer Matrix Method in Acoustics*, pp. 103–164. Cham: Springer International Publishing, 2021.

[18] J.-P. Groby, N. Jiménez, and V. Romero-García, *Acoustic Metamaterial Absorbers*, pp. 167–204. Cham: Springer International Publishing, 2021.

[19] M. Shibata and M. Nomura, "Lightweight covariance matrix adaptation evolution strategy (cma-es) implementation for python 3, https://pypi.org/project/cmaes/."

[20] C. R. Harris, K. J. Millman, and S. J. van der Walt et al., "Array programming with NumPy," *Nature*, vol. 585, pp. 357–362, Sept. 2020.

[21] P. Virtanen, R. Gommers, T. E. Oliphant, M. Haberland, and T. e. a. Reddy, "SciPy 1.0: Fundamental Algorithms for Scientific Computing in Python," *Nature Methods*, vol. 17, pp. 261–272, 2020.

[22] J.-P. Groby, R. Pommier, and Y. Aurégan, "Use of slow sound to design perfect and broadband passive sound absorbing materials," *The Journal of the Acoustical Society of America*, vol. 139, pp. 1660–1671, Apr. 2016.

[23] V. Romero-García, G. Theocharis, O. Richoux, and V. Pagneux, "Use of complex frequency plane to design broadband and sub-wavelength absorbers," *The Journal of the Acoustical Society of America*, vol. 139, pp. 3395–3403, June 2016.

[24] V. Romero-García, G. Theocharis, O. Richoux, A. Merkel, V. Tournat, and V. Pagneux, "Perfect and broadband acoustic absorption by critically coupled sub-wavelength resonators," *Scientific Reports*, vol. 6, Jan. 2016.